TEMPERATURE DEPENDENCE OF SILICON HARDNESS: EXPERIMENTAL EVIDENCE OF PHASE TRANSFORMATIONS

Vladislav Domnich[1], Yvonne Aratyn[2], Waltraud M. Kriven[2] and Yury Gogotsi[1]

[1]Department of Materials Science and Engineering and A.J. Drexel Nanotechnology Institute, Drexel University, Philadelphia, Pennsylvania 19104, USA
[2]Department of Materials Science and Engineering, University of Illinois at Urbana-Champaign, Urbana, Illinois 61801, USA

Abstract. The hardness of silicon is known to be nearly independent of temperature below a certain transition point, and to decrease steeply thereafter. Based on high-temperature Berkovich nanoindentation at 25–500 °C and Raman microanalysis of Vickers indentations produced in single-crystal silicon at 25–750 °C, we present evidence of a transformation into a high-pressure metallic Si phase during indentation at temperatures up to about 350 °C. We show that this transformation pressure determines silicon hardness below the transition temperature. We also report the temperature stability ranges of different metastable phases of silicon, including a new Si-XIII phase.

1. INTRODUCTION

It has been long recognized that the hardness vs. temperature dependence of silicon displays two distinctly different regions, the transition point between them roughly correlating with the Debye temperature for this material [1]. In particular, the experimental observations have shown that the hardness of silicon decreases by only ~5% from 25 to 350 – 500 °C [2-6] (shaded area in Fig. 1a), whereas above these temperatures, the decrease is much steeper, resembling a similar dependence commonly observed in metals [7] (Fig. 1a).

As shown in earlier works [1,6], the high-temperature indentation behavior of silicon can be quantitatively described by considering the dislocation motion in covalent crystals as a function of temperature and by relating the resulting values of the flow stress to the hardness. The governing equation,

$$\sinh \frac{\beta H}{T} = Ae^{U/kT} \qquad (1)$$

allows one to obtain an accurate fit to the experimental dependence of hardness H on temperature T above the transition point by varying the activation energy U and the fitting parameters A and β [6]. Combining this observation with the evidence of extensive dislocation activity in the vicinity of high-temperature imprints [5,6,8], Gilman [1] suggested that the hardness of Si above the transition point is determined by the activation energy for dislocation motion.

The prevailing mechanism of Si deformation below the transition temperature remains the subject of a controversial discussion in the literature. Limited dislocation activity has been reported on indents made at room temperature, and several dislocation-based theories (see [9] for a review) have been offered to explain the observed hardness *versus* temperature dependence in this region. Cracking has also been shown to contribute to the room-temperature deformation of silicon, particularly for indentations made at relatively high loads [2,10-12]. Finally, extensive experimental

---

Corresponding author: Yury Gogotsi, e-mail: gogotsi@drexel.edu
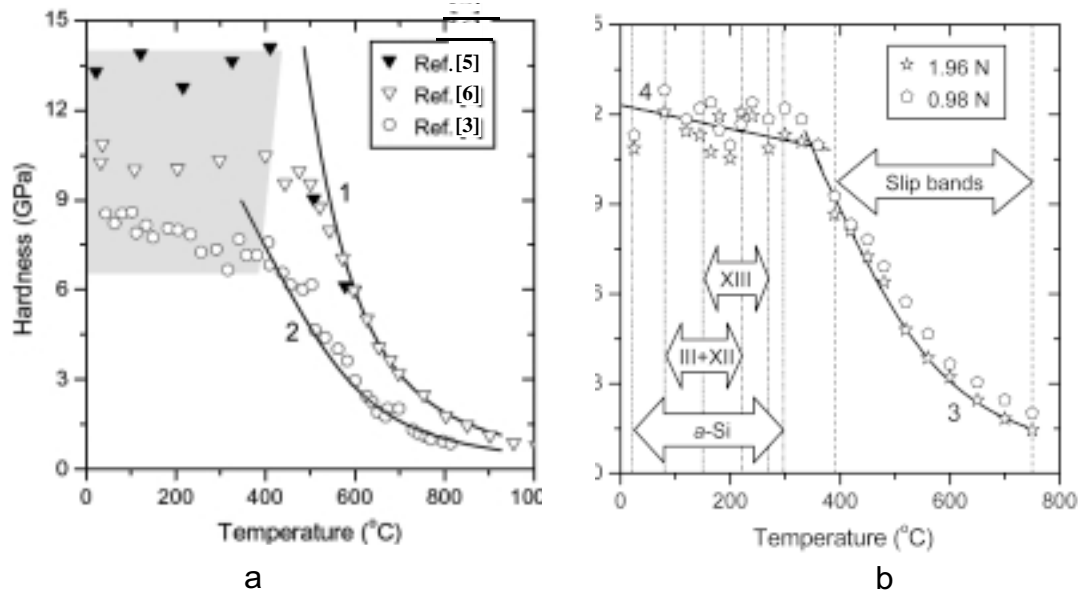
Fig. 1. Hardness vs. temperature dependencies in silicon: (a) compilation of literature data [3,5,6] and (b) our experiments. Solid lines (1–3) denote the calculated hardness due to dislocation glide according to Eq. (1), and (4) the calculated *cd* → β-tin transformation pressure for Si (Ref. [38], offset by 6 GPa). Arrows mark the temperature intervals in which various silicon phases were observed by Raman spectroscopy, and dislocation slip bands observed by optical microscopy. The existence of the *a*-Si, Si-III, Si-XII, and Si-XIII phases in hardness imprints indicates that the indentation-induced metallization of silicon occurs at these temperatures.

evidence [9,13-21] has indicated that silicon may also undergo phase transformations under a penetrating diamond indenter or in sliding contact.

From high-pressure cell experiments, it is known that the semiconducting cubic diamond silicon (Si-I or *cd*) transforms into a metallic phase with the β-tin structure (Si-II) at hydrostatic pressures of ~12 GPa. Upon slow unloading of Si-II, the formation of two semimetallic phases, the rhombohedral Si-XII or *r*8 and the body-centered cubic Si-III or *bc*8, has been reported. Although thermodynamically metastable, Si-III persists almost indefinitely at room temperature, due to extremely slow kinetics of its transformation to Si-I. At elevated temperatures, however, this kinetics is greatly enhanced and the Si-III → Si-I transition proceeds in the range of 200-600 °C through formation of an intermediate phase having the lonsdaleite (hexagonal diamond) structure, labeled as Si-IV or *hd* [9].

Observation of: (i) the Si-III and Si-XII phases in the residual imprints by Raman microspectroscopy [22,23] and transmission electron microscopy (TEM) [12-14,24,25], (ii) plastically extruded material around the indents [23,26], and (iii) a drop of indentation contact resistance [4,15,25,27-29], all point to the formation of metallic Si-II phase during indentation, similar to hydrostatic compression in the high-pressure cell. Further, noting a close correlation between the room-temperature hardness of silicon and the Si-I – Si-II transformation pressure, Gridneva *et al.* [4] suggested that Si hardness in the low-temperature region (Fig. 1a) is determined by the critical pressure required to initiate metallization of Si underneath the indenter, rather than by the activation energy for dislocation motion. According to this hypothesis, once a 12-GPa pressure threshold is reached in the contact zone and the Si-I → Si-II transformation has started, further loading will not lead to the increase of contact pressure and the measured hardness value, but rather to the expansion of the transformed metallic core into the surrounding material [1,4,30].

The structural investigation of indentations produced at elevated temperatures was performed by Suzuki and Ohmura [5], whose TEM images and the corresponding selected area diffraction patterns showed that the indents formed at room temperature were almost completely amorphized, the indents formed at 300 °C consisted of both amorphous material (*a*-Si) and Si-I, and the indents formed at 750 °C only contained some crystalline structures but no *a*-Si whatsoever. The authors attributed this observation to the formation of Si-II below the transition temperature and dislocation activity in Si-I above it. However, the evidence presented by Suzuki and Ohmura cannot be considered complete because no traces of the crystalline Si-III and Si-XII phases were observed in their experiments, and it can be argued that amorphous material formed directly from Si-I on loading by shear deformation [31], thus eliminating the metallic Si-II phase from the discussion.

Other studies reported the formation of Si-IV during indentation of silicon in the temperature range of 400 - 650 °C by twinning of the cubic diamond structure [8,32]. However, these studies were focused on characterization of the periphery of indents rather than the immediate contact zone, and therefore they are not relevant to the present discussion. In our own studies of thermal stability of the Si phases produced by nanoindentation [33], we observed transformation of Si-III and Si-XII into other structures at ~175 °C, starting with the formation of an unidentified crystalline phase labeled as Si-XIII. Upon further temperature increase, the observed transformation path was Si-XIII $\rightarrow$ Si-IV/ *a*-Si $\rightarrow$ nanocrystalline Si-I, eventually leading to the full recovery of Si-I at temperatures in excess of 600 °C.

A recent Raman spectroscopy study of Rockwell indents produced at high temperatures reported formation of various silicon polymorphs (Si-III, Si-IV, Si-XII, and amorphous silicon) inside the indented area [34], but the correlation with temperature dependence of hardness was not established in that study. Effect of temperature on phase transformations in Si continues to attract interest of researchers [35]. The most recent work suggested that Si-VIII phase may form at 100-125 °C [36]. However, the phase transformation routes are still not completely clear. We performed the experiments reported here in order to investigate the effect of heating on Si deformation underneath the sharp indenter, identify phase composition within the indents, and establish factors that determine the measured values of Si hardness in a wide range of temperatures.

2. EXPERIMENTAL

A Nikon QM high temperature microhardness tester equipped with a diamond Vickers indenter with the total included angle of 136° was used in these experiments. Heating was applied to both the indenter and the sample, and all measurements were carried out in vacuum (5.33$\cdot$10^{-3} Pa) to prevent silicon from oxidizing during exposure to high temperatures. The temperature was controlled to within ± 5 °C. Loading and unloading rates were not adjustable; the duration of a typical loading-unloading cycle was about 10 sec.

Pieces of polished and etched (111) single crystal Si wafers provided by Mitsubishi Silicon America were used. On each sample, a line of three indents at 0.98 N followed by three indents at 1.96 N was placed at room temperature (25 °C), after which the sample-indenter assembly was heated to the required temperature and a line of ten 0.98-N indents followed by ten 1.96-N indents was placed normal to the existing room-temperature indents. Overall, more than 200 indentations were produced in the temperature range of 25 to 750 °C.

The hardness was determined as an average contact pressure according to the expression

$$H = \frac{P}{A_{pro}} = \frac{2P}{d^2}, \qquad (2)$$

where P is the maximum applied load, A_{pro} is projected area of the indentation after unloading, and d is diagonal of the four-sided residual imprint as measured by scanning electron microscopy (SEM) and optical microscopy.

Raman spectroscopy was used for sample characterization after the indentation tests. A Ramascope 2000 microspectrometer (Renishaw, UK) equipped with an Ar-ion laser operating at 514.5 nm and an 100x objective was used, to enable the spatial resolution of ~1 μm. For *in situ* Raman microanalysis at elevated temperatures, a THMS 600 (Linkam, UK) hot stage was used. The stage allowed heating the samples up to 600 °C in argon atmosphere with simultaneous acquisition of the Raman spectra using a long working distance 50x objective with spatial resolution of ~2 μm. Temperature stability and sensor accuracy were within ±0.1 °C.

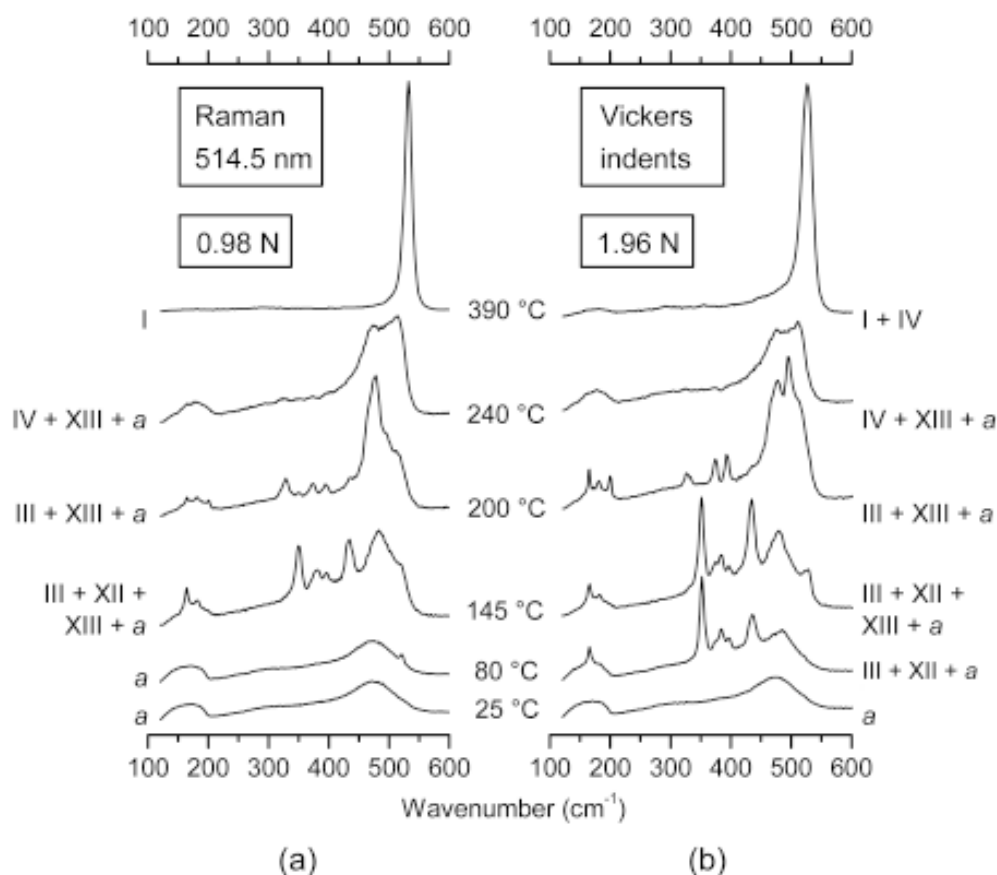Nanoindentation data were acquired with a diamond Berkovich indenter using a NanoTest sys-

Fig. 2. Raman spectra of Vickers indentations on silicon produced at elevated temperatures under loads of (a) 0.98 N and (b) 1.96 N. Broad features at 160 and 480 cm^{-1} indicate the presence of a-Si. The bands at 166, 184, 350, 375, 397, 435 and 485 cm^{-1} are assigned to Si-XII and the bands at 166, 384, 415, 433, 465 cm^{-1} to Si-III. Raman bands at 200, 330, 475, and 497 cm^{-1} are assigned to Si-XIII [9].

tem (Micro Materials, UK), equipped with a programmable heating stage with separate control of indenter and sample temperatures. Arrays of indentations were produced on (111) silicon wafers at temperatures of 25, 100, 200, 300, and 500 °C at the following conditions: loading to 50 mN at 1.67 mN/s, holding the maximum load for 5 s, and complete unloading at 0.56 mN/s. The nanoindentation hardness was measured using the standard Oliver and Pharr method [37].

3. RESULTS AND DISCUSSION

The temperature dependencies of Si hardness obtained in our experiments (Fig. 1b) were similar for both 0.98 N and 1.96 N loads and they showed a good agreement with the literature data shown in Fig. 1a. Differences in the absolute hardness val-

ues and the exact position of the transition point, as measured by different groups, could be attributed to variances in maximum loads and loading rates, indenter sharpness and/or surface finish of the samples. However, all data presented in Fig. 1 are consistent in showing the existence of two clearly demarkated regions in the $H(T)$ dependence. This made us confident that our results were compatible with the previous work and information about the phase composition of indents collected in our experiments should be applicable to explain the general behavior of silicon.

Fig. 2 shows typical Raman spectra of indentations made under 0.98 and 1.96-N loads in the temperature range of 25 to 390 °C. The spectra of both the smaller and the larger indents made at 25 °C show the presence of a-Si. This can be understood as the result of the fast unloading rates which could
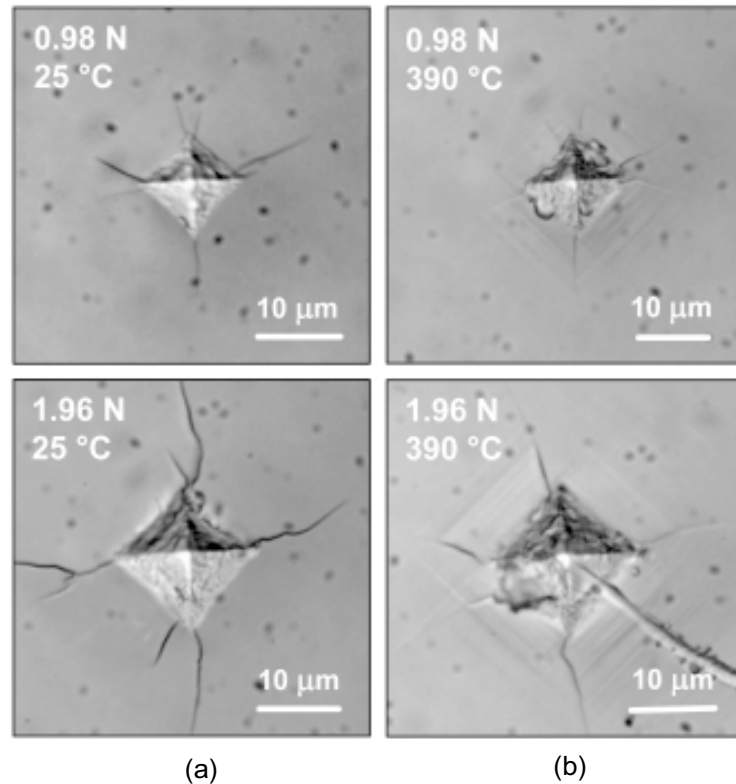
Fig. 3. Optical images of Vickers indentations produced on (111) silicon (a) at 25 °C and (b) 390 °C. Both imprints obtained at high temperature are surrounded by slip bands indicative of dislocation activity. Cracking around the indents was observed up to 550 °C.

not be controlled in our experiments. It has been shown that the Si-III and Si-XII phases form in indentations only after sufficiently slow unloading, while rapid unloading favors amorphization [19,23,24]. No such effect of the loading rate has been ever reported. Noteworthy is the fact that the formation of Si-III and Si-XII was observed in room-temperature Vickers indents in silicon made at the same loads as in our experiments, but under slower unloading conditions [19]. It is also important to note that the larger (1.96 N) indentation produced at 80 °C already shows the presence of the Si-III and Si-XII phases in addition to *a*-Si, whereas the smaller indent produced at the same temperature is still amorphous (Fig. 2). It is known from literature that higher applied loads promote the formation of the crystalline Si-III and Si-XII phases, while below a certain load threshold (depending on particular indentation geometry and unloading rates used), only amorphous material is observed [13,19,24].

The results of our Raman spectroscopy studies of indents made at 20 and 80 °C are therefore in good agreement with all previous observations, indicating the formation of Si-II during indentation. On unloading, the kinetically controlled Si-II → Si-XII transformation appears to take place only when sufficient time is allowed for nucleation of the new crystalline phase and subsequent lattice reconstruction. Rapid unloading rates favor gradual disordering of the Si-II lattice and lead to the formation of amorphous material. The probability of such a process should be sensitive to temperature and the available volume of the transforming material, which is in agreement with our observations shown in Fig. 2.

At 145 °C, both indentations are already a mixture of Si-III, Si-XII, Si-XIII, and *a*-Si (Fig. 2). Moreover, Si-XIII becomes a predominant phase in the samples indented at 200 °C. The Raman spectrum of Si-XIII has four characteristic lines at 200, 330,
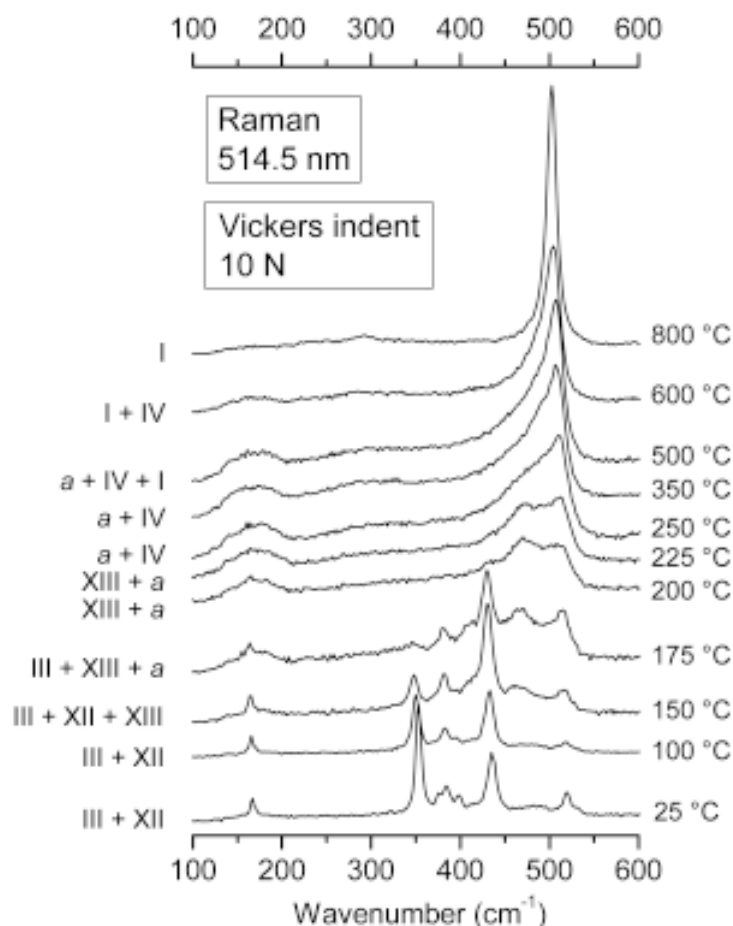
Fig. 4. Effect of annealing on the Raman spectra of a 10-N Vickers microindentation on silicon. The transition path is identical to that of Fig. 2.

475, and 497 cm^{-1}, which do not match any of the established spectra of various Si phases [9]. The fact that these lines are narrow implies that they originate from a crystalline structure. So far, the formation of Si-XIII has been confirmed by means of Raman spectroscopy [9] with only some TEM evidence provided later [33]. The exact crystal structure of this phase is still to be determined. Although very sensitive to overheating, the Si-XIII phase proved to be rather stable within the residual imprints at ambient conditions; in fact, the Raman spectra of some samples displaying Si-XIII did not change over the two-year period.

As the testing temperatures were increased further, a series of transitions Si-XIII → Si-IV → Si-I was monitored (Fig. 2). The spectra of imprints made at 390 °C show the presence of the Si-I phase only (Fig. 2), and similar spectra were collected

from all imprints made at higher temperatures, up to 750 °C. Further, optical microscopy analysis of the indented samples revealed the presence of characteristic fringes around the imprints made at temperatures of 390 °C and higher (Fig. 3b), usually considered an indication of dislocation activity that accommodates plastic deformation. No such features were observed around indentations made at lower temperatures (Fig. 3a). Therefore, both Raman spectroscopy and optical microscopy results suggest that a change in the deformation mode of silicon occurs around 350 °C in our experiments.

The presence of amorphous material and metastable crystalline phases within indentations made at temperatures below 350 °C indicates formation of Si-II during loading. By comparing our hardness-temperature data with the temperatures at which
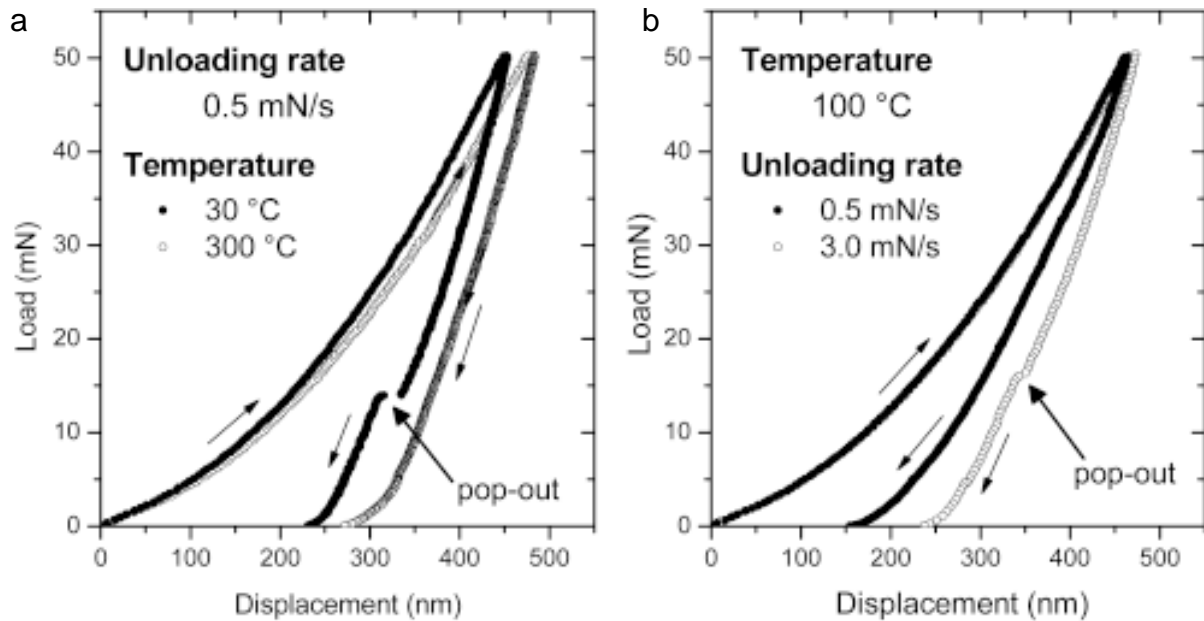
Fig. 5. Nanoindentation load-displacement curves produced on (111) silicon at (a) RT and 300 °C and (b) at 100 °C and loading rate of 0.55 and 3 mN/s using a Berkovich diamond indenter. The displacement discontinuity in the unloading curve ("pop-out") is an indication of a phase transition during pressure release [22].

the metastable phases, including *a*-Si, are formed (Fig. 1b), it is immediately recognized that the extent of phase transformations and hence the indentation-induced metallization of silicon correlates with the athermal region in its hardness-temperature dependence. Moreover, the theoretically predicted phase boundary between the cubic diamond and the β-tin structures in Si exhibits a slightly declining slope with increasing temperature [38], and this trend is again in agreement with our experimental hardness data (see line 4 in Fig. 1b).

Above ~350 °C, only cubic diamond silicon was observed by Raman spectroscopy and the evidence of dislocation gliding in Si-I was given by optical microscopy. This implies that in this temperature range, silicon underneath the indenter deforms by dislocation-induced plastic flow rather then pressure-induced metallization. Indeed, the temperature-dependent region of our hardness data closely correlates with the calculated flow stress in Si due to the dislocation glide given by Eq. (1) (line 3 in Fig. 1b).

It is interesting to note that similar results were obtained by *in situ* Raman microanalysis of Vickers indentations made in silicon at room temperature and then heated in the Ar-purged chamber con-

nected to a Raman spectrometer (Fig. 4). In this case, the heating rates were relatively fast (on the order of 1 degree per second), but longer acquisition times were required to collect meaningful data (typically, 20-40 minutes per each spectrum in Fig. 4). The evolution of the Raman spectra during heating shown in Fig. 4 is almost identical to that in Fig. 2, which clearly indicates that the temperature-assisted transformation of the residual Si-III and Si-XII phases into the thermodynamically stable Si-I follows similar routes for indentations made at elevated temperatures and those made at ambient conditions and annealed afterwards.

Additional information can be extracted from analysis of nanoindentation load-displacement curves produced in the same silicon wafer at different temperatures (Fig. 5). A displacement discontinuity in the unloading curve ("pop-out"), seen in Fig. 5a for an indentation made at RT, is commonly interpreted as an abrupt transformation from the Si-II to the Si-XII phase on pressure release [22]. The pop-out can be observed in 100 and 200° curves, but at high unloading rates (Fig. 5b), because the transformation of metastable phases occurs continuously during slow unloading leading to a large elastic recovery and lower residual dis-

placement (Fig. 5b). In contrast, at higher temperatures, as the typical 300 °C indentation data shown in Fig. 5a displays, no such discontinuity could be observed, and the load-displacement curves are similar to those of a regular elastoplastic material without phase changes [37]. This is again in excellent agreement with our Raman data for microindentations produced at the same temperatures. Moreover, the nanoindentation hardness measured from the load-displacement curves shown in Fig. 5 was in the range of 12-14 GPa for indentations in the temperature range of 25 - 300 °C, and began to decrease thereafter, in agreement with the plots shown in Fig. 1. This provides further evidence that phase transformations are an important deformation mechanism that determines silicon hardness at temperatures below a transition point.

Clearly, cracking contributes significantly to Si deformation under indentation, particularly at lower temperatures and higher indentation loads (see Fig. 3). In fact, surface cracks were observed around indents made at temperatures up to 550 °C in our experiments, extending far beyond the athermal region in the hardness-temperature dependence (Fig. 1b). Also, limited dislocation activity around the clearly demarcated transformation zone has been reported for room-temperature Si indents [10,12-14,24]. This suggests that indentation-induced metallization of Si below the transition point is accompanied by brittle fracture and confined plastic flow, in order to partially accommodate high strains in the surrounding material.

4. CONCLUSIONS

In this research, we give experimental evidence that phase transformations are taking place during indentation of silicon in the temperature range of 25 - 300 °C, under a variety of experimental conditions. In particular, we argue that up to 300-350 °C, the measured hardness of silicon is determined by pressure required to transform the semiconducting Si-I phase into the metallic Si-II. Above this temperature, no phase transformations are observed and the hardness of Si is determined primarily by dislocation glide in Si-I. Further, the temperature range for formation of a new Si-XIII phase has been identified, and crystallographic work on structural identification of this phase will follow.

A complete understanding of the temperature dependence of phase changes induced by contact loading is important for emerging high-temperature applications of Si, such as fabrication of a micro

gas turbine engine. However, the fundamental importance of our findings extends beyond Si alone. Our comparison of the "athermal" region of the hardness dependence for Ge with the temperature dependence of the metallization pressure [38] shows an excellent agreement, similar to that observed for Si (Fig. 1b). We believe that further experimental work, including Raman spectroscopy and TEM studies of hot-hardness indents, will help explain similar temperature dependences of hardness for other semiconductors, diamond [39] and ceramics [40, 41] from the same perspective.

ACKNOWLEDGEMENTS

REFERENCES

[1] J. J. Gilman // *Science* **261** (1993) 1436.
[2] P. Feltham and R. Banerjee // *J. Mater. Sci.* **27** (1992) 1626.
[3] J. J. Gilman // *J. Appl. Phys.* **46** (1975) 5110.
[4] I. V. Gridneva, Y. V. Milman and V. I. Trefilov // *Phys. Stat. Sol. (a)* **9** (1972) 177.
[5] T. Suzuki and T. Ohmura // *Philos. Mag. A* **74** (1996) 1073.
[6] V. I. Trefilov and Y. V. Milman // *Sov. Phys. Dokl.* **8** (1964) 1240.
[7] D. Tabor // *Philos. Mag. A* **75** (1996) 1207.
[8] V. G. Eremenko and V. I. Nikitenko // *Phys. Stat. Sol.* (a) **14** (1972) 317.
[9] V. Domnich and Y. Gogotsi // *Rev. Adv. Mater. Sci.* **3** (2002) 1.
[10] T. F. Page, W. C. Oliver and C. J. McHargue // *J. Mater. Res.* **7** (1992) 450.
[11] R. W. Armstrong, H. Shin and A. W. Ruff // *Mat. Sci. Eng. A* **209** (1996) 91.
[12] H. Saka, A. Shimatani, M. Suganuma and Suprijadi // *Phil. Mag. A* **82** (2002) 1971.
[13] I. Zarudi and L. C. Zhang // *Trib. Int.* **32** (1999) 701.
[14] D. Ge, V. Domnich and Y. Gogotsi // *J. Appl. Phys.* **93** (2003) 2418.
[15] J. E. Bradby, J. S. Williams and M. V. Swain // *Phys. Rev.* B **67** (2003) 085205.
[16] Y. Gogotsi, C. Baek and F. Kirscht // *Semicond. Sci. Tech.* **14** (1999) 928.

[17] Y. Gogotsi, G. Zhou, S.-S. Ku and S. Cetinkunt // *Semicond. Sci. Technol*. **16** (2001) 345.

[18] A. Kovalchenko, Y. Gogotsi, V. Domnich and A. Erdemir // *Tribology Transactions* **45** (2002) 372.

[19] T. Juliano, Y. Gogotsi and V. Domnich // *Journal of Materials Research* **18** (2003) 1192.

[20] T. Juliano, V. Domnich and Y. Gogotsi // *Journal of Materials Research* **19** (2004) 3099.

[21] Y. G. Gogotsi, K. G. Nickel and A. Kailer // *Mater. Res. Innovat* **1** (1997) 3.

[22] V. Domnich, Y. Gogotsi and S. Dub // *Appl. Phys. Lett*. **76** (2000) 2214.

[23] A. Kailer, Y. G. Gogotsi and K. G. Nickel // *J. Appl. Phys*. **81** (1997) 3057.

[24] J. E. Bradby, J. S. Williams, J. Wong-Leung, M. V. Swain and P. Munroe // *J. Mater. Res.* **16** (2001) 1500.

[25] A. B. Mann, D. van Heerden, J. B. Pethica and T. P. Weihs // *J. Mater. Res*. **15** (2000) 1754.

[26] G. M. Pharr, W. C. Oliver and D. S. Harding // *J. Mater. Res.* **6** (1991) 1129.

[27] D. R. Clarke, M. C. Kroll, P. D. Kirchner, R. F. Cook and B. J. Hockey // *Phys. Rev. Lett.* **60** (1988) 2156.

[28] M. C. Gupta and A. L. Ruoff // *J. Appl. Phys*. **51** (1980) 1072.

[29] G. M. Pharr, W. C. Oliver, R. F. Cook, P. D. Kirchner, M. C. Kroll, T. R. Dinger and D. R. Clarke // *J. Mater. Res*. **7** (1992) 961.

[30] A. P. Gerk and D. Tabor // *Nature* **271** (1978) 732.

[31] Y. Q. Wu and Y. B. Xu // *J. Mater. Res*. **14** (1999) 682.

[32] P. Pirouz, R. Chaim, U. Dahmen and K. H. Westmacott // *Acta Metall. Mater*. **38** (1990) 313.

[33] D. Ge, V. Domnich and Y. Gogotsi // *Journal of Applied Physics* **95** (2004) 2725.

[34] S. Kouteva-Arguirova, V. Orlov, W. Seifert, J. Reif and H. Richter // *The European Physical Journal Applied Physics* **27** (2004) 279.

[35] S. Ruffell, J. E. Bradby, N. Fujisawa and J. S. Williams // *Journal of Applied Physics* **101** (2007) 083531.

[36] R. K. Singh, P. Munroe and M. Hoffman // *J. Mater. Res*. **23** (2008) 245.

[37] W. C. Oliver and G. M. Pharr // *J. Mater. Res.* **7** (1992) 1564.

[38] K. Gaal-Nagy, A. Bauer, M. Schmitt, K. Karch, P. Pavone and D. Strauch // *Phys. Stat. Sol. (b)* **211** (1999) 275.

[39] Y. G. Gogotsi and K. G. N. A. Kailer // *J. Appl. Phys*. **84** (1998) 1299.

[40] V. Domnich, Y. Gogotsi, M. Trenary and T. Tanaka // *Applied Physics Letters* **81** (2002) 3783.

[41] D. Ge, V. Domnich, T. Juliano, E. Stach and Y. Gogotsi // *Acta Materialia* **52** (2004) 3921.